

SHORT PAPER

Threshold-Based Segmentation for Landmark Detection Using CBCT Images

Mohammed

Ed-dhahraouy¹(✉),Hicham Riri¹, ManalEzzahmouly¹, AbdelmajidElmoutaouakkil¹, FaridBourzgui², Hamid El Byad¹¹Chouaib Doukkali University,
El Jadida, Morocco²University Hassan 2,
Casablanca, Moroccodahraouimed89@gmail.com**ABSTRACT**

The aim of this study is to examine the influence of threshold-based segmentation on the mean error of automatic landmark detection in 3D CBCT images. A GUI was developed for radiologists, allowing manual landmark identification and visualization of CBCT images. After a threshold-based segmentation, a semi-automatic algorithm for landmark detection was designed using the anatomic definition of each landmark. A step of 50 Hounsfield units was used for threshold variation to assess the detection error. 5 CBCT images were used to validate the proposed approach. The measurement of error detection for one patient was influenced by the threshold variation. For this patient, the error changed from 1.49 mm to 10.32 mm at a low threshold value, while for another patient, the error changed from 1.96 mm to 12.28 mm at high a threshold value. In a CBCT scanner, the choice of threshold value for segmentation can be an important factor in causing error in measurements.

KEYWORDS

CBCT image, landmark detection, segmentation, 3D cephalometry

1 INTRODUCTION

For many years, radiographs have been considered important for various orthodontic applications such as malocclusion, facial structure asymmetry, and cephalometric analysis. However, a radiographic image is a 2D representation of the 3D structure and does not show precise anatomic information, which reduces the measurement accuracy. This limitation has been eliminated with the introduction of the cone beam computed tomography (CBCT) imaging technique. Using CBCT technology allows us to obtain an accurate depiction of the anatomical configuration. Recently, many research groups have addressed the use of CBCT in 3D cephalometry to overcome the limitations of 2D cephalometry [1–3]. A few researchers have proposed automatic and semi-automatic algorithms for landmark detection in 3D cephalometry [4–7], [9–12]. In the literature, there are three main methods employed for automatic 3D cephalometry: model-based [4–5, 7],

Ed-dhahraouy, M., Riri, H., Ezzahmouly, M., Elmoutaouakkil, A., Bourzgui, F., Byad, H.E. (2023). Threshold-Based Segmentation for Landmark Detection Using CBCT Images. *International Journal of Online and Biomedical Engineering (iJOE)*, 19(10), pp. 169–176. <https://doi.org/10.3991/ijoe.v19i10.39489>

Article submitted 2023-03-09. Resubmitted 2023-04-27. Final acceptance 2023-04-27. Final version published as submitted by the authors.

© 2023 by the authors of this article. Published under CC-BY.

deep-learning [13], and knowledge-based strategies [6, 9, 12]. Convolutional neural networks (CNNs) have shown great potential in medical image analysis, especially in landmark detection. CNNs can automatically learn high-level features from input images and perform well on new images with similar properties. However, the success of CNN-based techniques is heavily dependent on the amount and type of training data, network architecture, and optimization algorithm used [14–15]. No previous work has addressed the influence of threshold-based segmentation on the automatic localization of landmarks in 3D cephalometry. In this paper, we propose a semi-automatic algorithm for landmark detection and then study the impact of the threshold values on the detection error.

2 MATERIALS AND METHODS

Five mandibles were used in this study. The scan of each mandible was obtained by a CBCT scanner (Newtom 3G-QR, Inc., Verona, Italy) for other diagnostic reasons independent of this study.

Each 3D dataset was used in digital imaging and communication in medicine (DICOM) format with 609 2D slices (512×512 of spatial resolution) and a voxel resolution of 0.3 mm. A user interface tool was used to visualize and render 3D images. As stated in a previous study [8], there are many techniques for rendering 3D volumes. In this work, we adopted the marching cube as a reconstruction algorithm for 3D surfaces. An overview of the proposed methodology is presented in Figure 1.

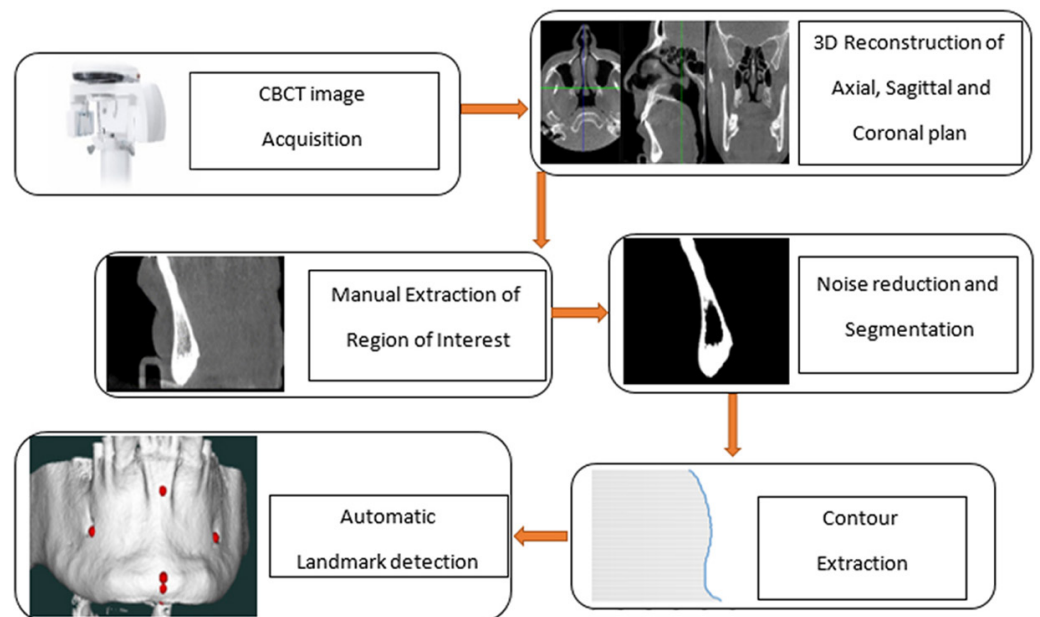


Fig. 1. Overview of the proposed methodology for landmark detection

2.1 Automatic landmark detection

Mental foramen (MfR–MfL). The program located the left mental foramen (MfL) first, and then, with the same method, the right mental foramen (MfR) was detected. For the MfL, the algorithm started with contour detection for each slice

in the axial plane on the left side of the seed point. Figure 2 shows an example of contour detection with MfL. To detect MfL, the program calculates the distance between the y-axis of point (i) and the y-axis of point (i+1) until it finds a negative distance, which indicates the existence of MfL.

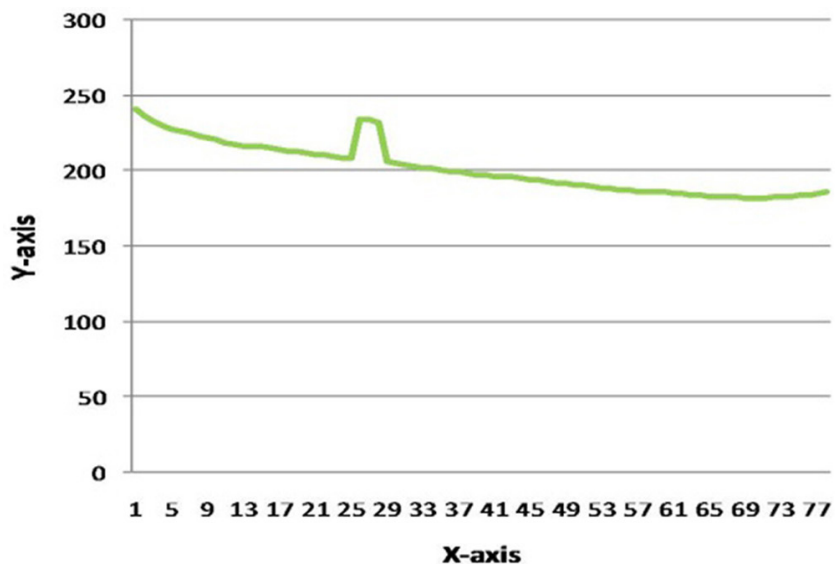


Fig. 2. Contour detection in the slice that contains MfL

Landmark: Menton (Me), Gnathion (Gn), Pogonion (Pog) and B-point (B).

These landmarks are located in the midline of the symphysis menti. In order to detect the contour of the symphysis menti structure, an operator selects the region of interest (ROI) in the midsagittal plane. In our study, a 3D contour was extracted and then the 3D coordinates (x, y, and z) of each landmark were generated by the algorithm. The detection of the four landmarks is based on the anatomic definition of each landmark. Table 1 shows the definitions of all landmarks.

Table 1. Definitions of anatomical landmarks

No.	Landmark	Definition
1	Menton: Men	Menton is the most inferior midpoint of the chin on the outline of the mandibular symphysis.
2	Gnathion: Gn	Gnathion is the most anterior and inferior point on the contour of the mandibular symphysis.
3	Pogonion: Pog	Pogonion is the most anterior midpoint of the chin on the outline of the mandibular symphysis.
4	B-Point: B	B-Point is the point of maximum concavity in the mid-line of the alveolar process of the mandible.
5-6	Mental foramen (MfR-MfL)	MF is below the apex of the second premolar.

2.2 Impact of segmentation on error detection

In this section, we describe our method used to investigate the impact of threshold-based segmentation on the error detection of the automatic algorithm.

Figure 3 presents the algorithm of threshold variation. The reference threshold value is critical for segmentation since it separates hard tissue from soft tissue. The algorithm took as input the expert threshold (ET), and then a step of 50 HU was used for threshold variation. Four steps above and four below the ET were used in this study.

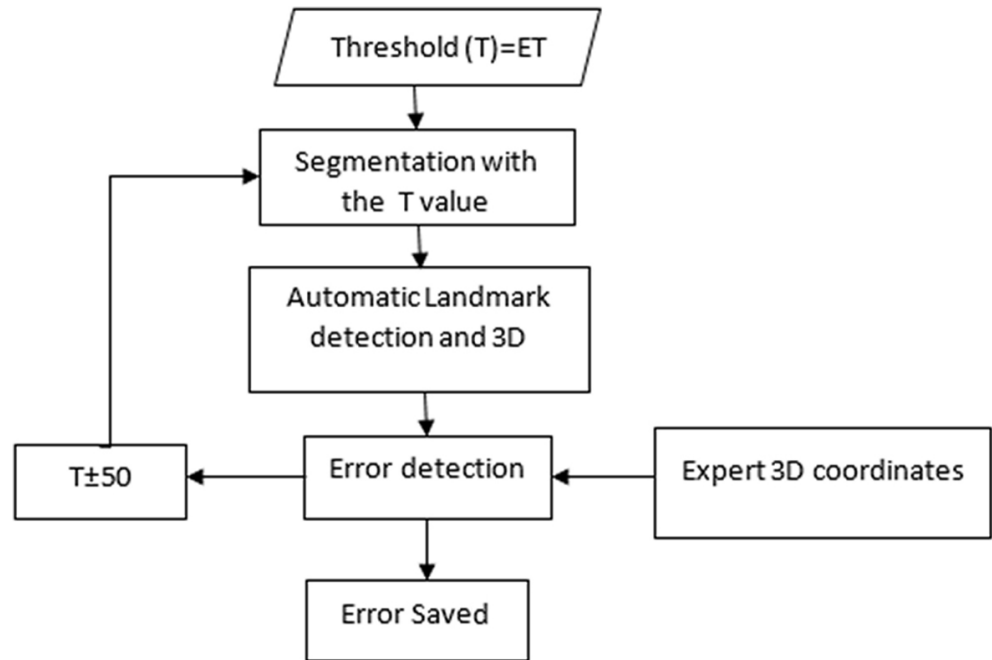


Fig. 3. Method used to study the impact of threshold variation

3 RESULTS

Table 2 shows the error detection for each threshold value. The error presented is the average error of the six landmarks detected. The range of threshold variation is between ET-200 and ET+200 with a step of 50 HU. The reference threshold selected by the expert was 890 HU for all patients.

Table 2. Detection error in mm for each threshold value

CBCT image	ET-200	ET-150	ET-100	ET-50	ET	ET+50	ET+100	ET+150	ET+200
1	10.32	1.10	1.39	1.33	1.49	1.46	1.55	1.55	1.55
2	2.53	2.09	2.04	1.81	1.92	2.93	2.08	2.16	2.25
3	2.62	2.64	2.64	2.67	2.71	2.78	2.78	2.58	2.58
4	1.89	1.84	1.86	1.90	1.96	1.95	2.25	12.28	12.28
5	2.79	2.83	2.90	3.26	2.97	4.13	4.24	4.23	4.23
Mean Error	4.03	2.10	2.17	2.19	2.21	2.65	2.58	4.56	4.58

These results show no significant difference in error detection between different thresholds except for ET-200 in patient 1 and (ET+150, ET+200) in patient 4. Figure 4 shows some examples of extracted contours.

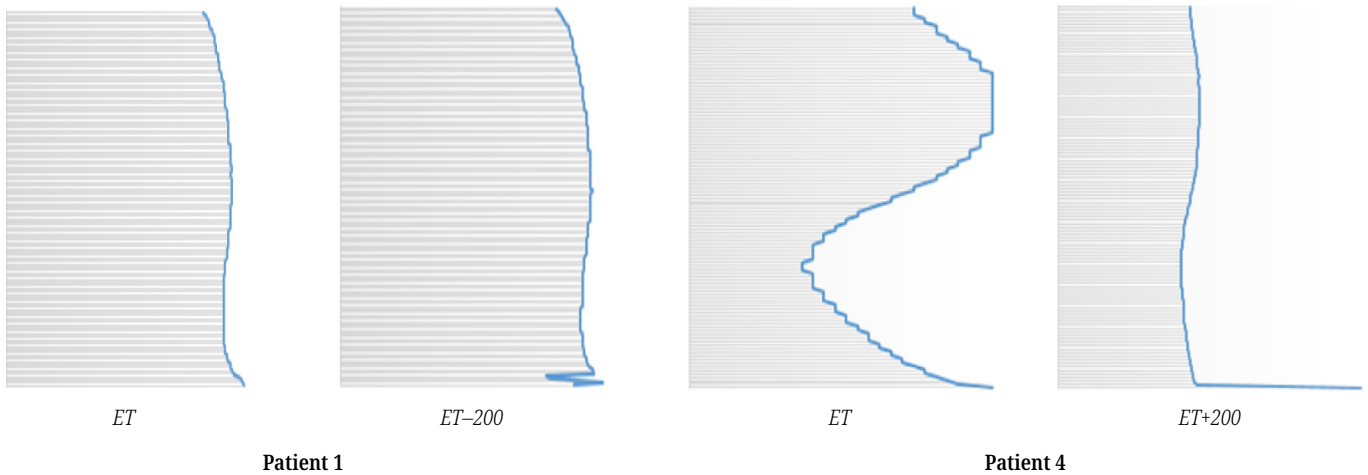


Fig. 4. Examples of contour detection by variation in threshold

Figure 4 provides the form of the extracted contour. There is a significant difference between the two forms of contours in each patient, which explains the difference in error detection in patients 1 and 4.

4 DISCUSSION

This study aimed at investigating the impact of threshold-based segmentation on automatic landmark detection located on the hard tissue of the mandible structure. The proposed approach was capable of detecting six landmarks and studying the correlation between error detection and the threshold value used for segmentation. Table 2 shows that the error in the first CBCT image became higher (10.32 mm) at the threshold value ET-200. This error is explained by the appearance of noise in the image at a low threshold value. Figure 4 shows the change in the contour form due to noise. Figure 5 presents an original slice and the result of segmentation with two different threshold values.

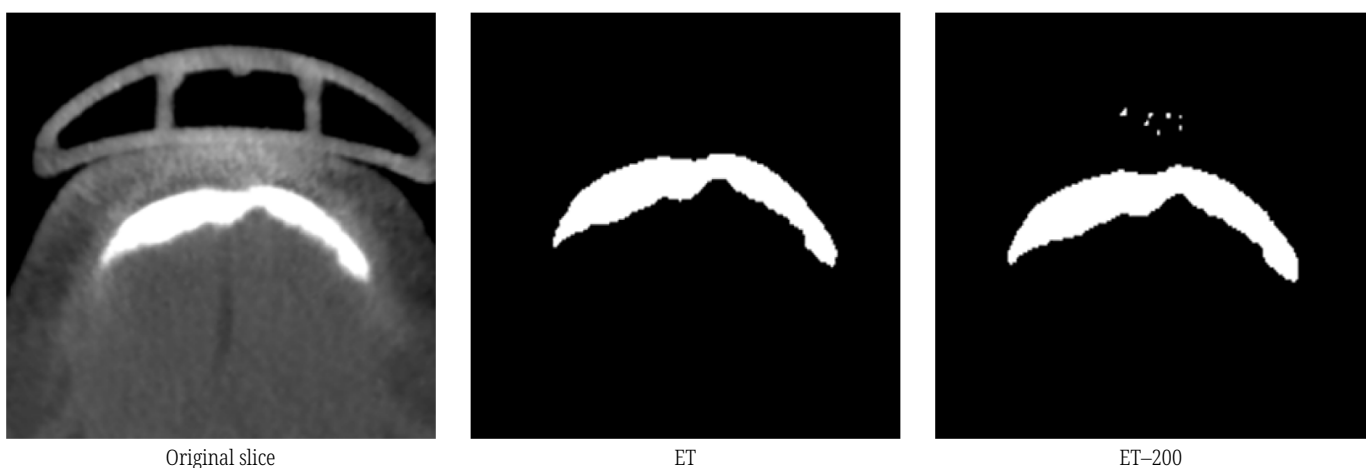


Fig. 5. Effect of threshold value on the appearance of noise in CBCT image 1

The higher value of error detection (12.28) for ET+150 and ET+200 in CBCT image 4 is attributed to the change in bone structure, as shown in Figure 6. The same landmark (Menton) was successfully detected at value ET but disappeared for values of ET+150 and higher.

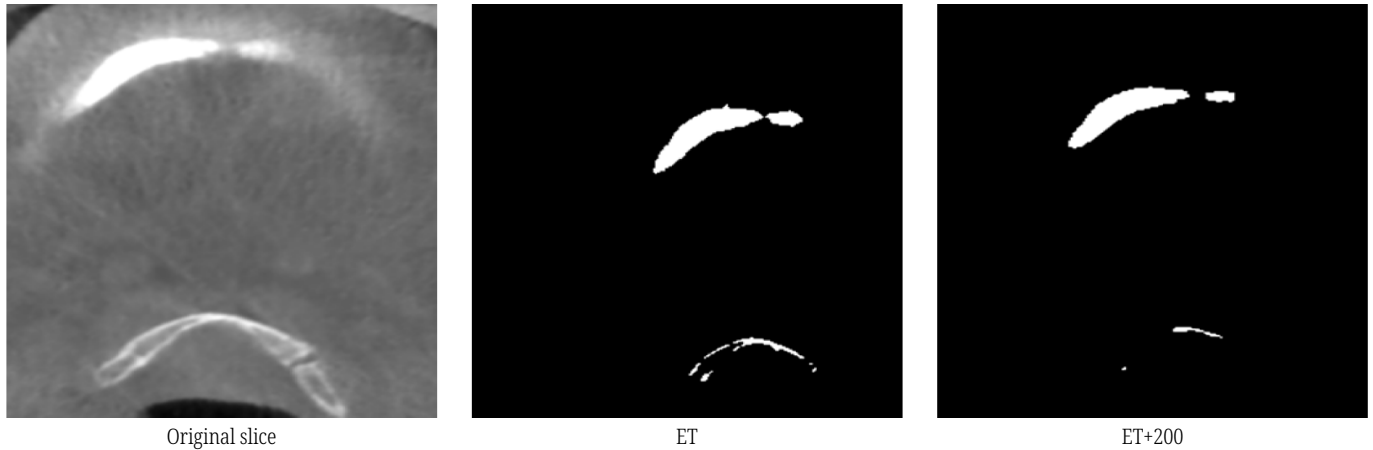


Fig. 6. Influence of threshold value on bone structure in CBCT image 4

A few studies have attempted to provide algorithms for automatic or semi-automatic landmark detection in 3D cephalometry [4–7], [12–13]. The aim of this study is to show the influence of threshold-based segmentation on automatic landmark detection. The results of error detection in this study can be compared to the results of error detection in previous studies. The range error was between 1.99 mm and 3.40 mm in all previous studies, while in the current study, the best mean error was 2.10 mm at threshold ET–150 and the worst was 4.58 mm at the extreme threshold value ET+200. Therefore, threshold-based segmentation could be an important factor that affects the mean error. The results of this work demonstrated that the choice of threshold value for segmentation can be critical in automatic landmark detection using a CBCT scanner.

5 CONCLUSION

The main objective of this study was to examine the threshold value used for segmentation and its impact on the mean error of detection. The finding of the current study was that the mean error was significantly higher at some high and low threshold values, even though the algorithm for landmark detection shows consistency for some images. To tackle the issue of automation, further research is needed for the preprocessing and segmentation of CBCT images.

6 REFERENCES

- [1] Swennen GRJ, Schutyser F, Barth E, De Groeve P, De Mey A. A new method of 3-D cephalometry Part I: the anatomic Cartesian 3-D reference system. *J Craniofac Surg.* 2006;17(2):314–25. <https://doi.org/10.1097/00001665-200603000-00019>

- [2] Chien PC, Parks ET, Eraso F, Hartsfield JK, Roberts WE, Ofner S. Comparison of reliability in anatomical landmark identification using two-dimensional digital cephalometrics and three-dimensional cone beam computed tomography in vivo. *Dentomaxillofacial Radiol.* 2009;38(5):262–73. <https://doi.org/10.1259/dmfr/81889955>
- [3] Hassan B, Van Der Stelt P, Sanderink G. Accuracy of three-dimensional measurements obtained from cone beam computed tomography surface-rendered images for cephalometric analysis: Influence of patient scanning position. *Eur J Orthod.* 2009;31(2):129–34. <https://doi.org/10.1093/ejo/cjn088>
- [4] Codari M, Caffini M, Tartaglia GM, Sforza C, Baselli G. Computer-aided cephalometric landmark annotation for CBCT data. *Int J Comput Assist Radiol Surg.* 2017;12(1):113–21. <https://doi.org/10.1007/s11548-016-1453-9>
- [5] Makram M, Kamel H. Reeb graph for automatic 3D cephalometry. *Int J Image Process* 2014;8:17–29.
- [6] Gupta A, Kharbanda OP, Sardana V, Balachandran R, Sardana HK. A knowledge-based algorithm for automatic detection of cephalometric landmarks on CBCT images. *Int J Comput Assist Radiol Surg.* 2015;10(11):1737–52. <https://doi.org/10.1007/s11548-015-1173-6>
- [7] Shahidi S, Bahrampour E, Soltanimehr E, Zamani A, Oshagh M, Moattari M. The accuracy of a designed software for automated localization of craniofacial landmarks on CBCT images. *BMC Med Imaging* 2014;1–8. <https://doi.org/10.1186/1471-2342-14-32>
- [8] Mady AS, Abou El-Seoud S. An overview of volume rendering techniques for medical imaging. *Int J Onl Eng.* 2020;16(6):95–106. <https://doi.org/10.3991/ijoe.v16i06.13627>
- [9] Ed-Dhahraouy M, Riri H, Ezzahmouly M, Bourzgui F, El Moutaoukkil A. A new methodology for automatic detection of reference points in 3D cephalometry: A pilot study. *International Orthodontics* 2018;16(2):328–337. <https://doi.org/10.1016/j.ortho.2018.03.013>
- [10] Zhang J, et al. Automatic craniomaxillofacial landmark digitization via segmentation-guided partially-joint regression forest model and multi-scale statistical features. *IEEE Trans Biomed Eng.* 2016;63(9):1820–1829. <https://doi.org/10.1109/TBME.2015.2503421>
- [11] Adams GL, Gansky SA, Miller AJ, Harrell WE, Hatcher DC. Comparison between traditional 2-dimensional cephalometry and a 3-dimensional approach on human dry skulls. *Am J Orthod Dentofac Orthop.* 2004;126(4):397–409. <https://doi.org/10.1016/j.ajodo.2004.03.023>
- [12] Ed-dhahraouy M, Riri H, Ezzahmouly M, Moutaouakkil AE, Aghoutan H, Bourzgui F. Proposition of local automatic algorithm for landmark detection in 3D cephalometry. *Bulletin of Electrical Engineering and Informatics* 2021;10(2):707–715. <https://doi.org/10.11591/eei.v10i2.1827>
- [13] Kang SH, Jeon K, Kang S-H, Lee S-H. 3D cephalometric landmark detection by multiple stage deep reinforcement learning. *Sci Rep.* 2021;11(1):17509. <https://doi.org/10.1038/s41598-021-97116-7>
- [14] Kadhim ZS, Abdullah HS, Ghathwan KI. Artificial neural network hyperparameters optimization: A survey. *Int J Onl Eng.* 2022;18(15):59–87. <https://doi.org/10.3991/ijoe.v18i15.34399>
- [15] Hoque ME, Kipli K. Deep learning in retinal image segmentation and feature extraction: A review. *Int J Onl Eng.* 2021;17(14):103–118. <https://doi.org/10.3991/ijoe.v17i14.24819>

7 AUTHORS

Mohammed Ed-dhahraouy received a PhD degree in medical image processing from Chouaib Doukkali University, El Jadida, Morocco, in 2019. Currently he is a researcher in the Laboratory of Optimization, Emerging Systems, Networks and Imaging, Computer Science Department, Chouaib Doukkali University, El Jadida, Morocco (email: dahraouimed89@gmail.com).

Hicham Riri received a PhD degree in medical image processing from Chouaib Doukkali University, El Jadida, Morocco, in 2020. Currently he is a researcher in the Laboratory of Optimization, Emerging Systems, Networks and Imaging, Computer Science Department, Chouaib Doukkali University, El Jadida, Morocco.

Manal Ezzahmouly received a PhD in medical image processing from Chouaib Doukkali University. She is a computer engineer from the Mohamed VI International Academy of Civil Aviation. Currently she is part of the team of Optimization, Emerging Systems, Networks and Imaging Laboratory, Computer Science Department, Chouaib Doukkali University, El Jadida, Morocco. Her research work focuses on the advanced processing of medical images.

Abdelmajid Elmoutaouakkil received a PhD in medical image processing and Electrical Engineering and Industrial Computing from INSA, Lyon, France, in 1995. He is a Professor of Computer Science and currently is part of the team of Optimization, Emerging Systems, Networks and Imaging Laboratory, Computer Science Department, Chouaib Doukkali University, El Jadida, Morocco.

Farid Bourzgui is Professor in the Faculty of Dental Medicine in Casablanca and Head of the Dento-Facial Orthopedic Department in the Faculty of Dentistry at University Hassan 2, Casablanca, Morocco.

Hamid El Byad received a PhD in dental medicine from the Faculty of Dental Medicine at University Hassan 2, Casablanca in 1995. He is a practical implantologist in a medical center in Casablanca, Morocco.